

The variability of equatorial thermocline spreading as an indication of equatorial upwelling in the Atlantic Ocean

Eberhard FAHRBACH (1) and Eduard BAUERFEIND (1)

ABSTRACT

From February to June 1979 ten sections with STD-measurements and nutrient casts were carried out by the West German R.V. "Meteor" in the equatorial Atlantic along 22° W between 2° S and 3° N. During part of this time current meters were moored. This data set is used to study the vertical spreading of isolines in the thermocline level which is observed near the equator. The spreading is similar for physical and chemical quantities. It could be caused by two mechanisms: the meridionally increased vertical mixing due to the high current shear between the South Equatorial Current and the Equatorial Undercurrent or meridional circulation cells, representing equatorial upwelling. The influence of the different processes is compared by calculating the terms of the equation of heat conservation. We find that vertical mixing is high enough to balance the heat gain of the ocean, but the comparison of periods with strong and weak spreading shows that the increased vertical mixing coefficient is compensated by a smaller vertical second derivative. Therefore the presence of equatorial upwelling is claimed to explain the observed local temperature change. The vertical advection is estimated from the horizontal divergence. As the zonal component of the divergence cannot be calculated from the data, it is derived under the hypothetical assumption of a 25 day period wave. Comparison with the observed local time change of temperature indicates that the vertical velocity is estimated too high. It is corrected to fit the observed temperature change. A vertical velocity of 3.4 m/d results during an upwelling event. It is concluded that there is a continuous spreading due to vertical mixing which is enhanced by vertical advection during upwelling events.

KEY WORDS : Equatorial upwelling — Thermocline spreading -- Vertical mixing - Vertical advection -- STD-, nutrient- and current measurements.

RÉSUMÉ

**LA VARIABILITÉ DE L'ÉTALEMENT DE LA THERMOCLINE À L'ÉQUATEUR COMME INDICATEUR D'UPWELLING
ÉQUATORIAL DANS L'OcéAN ATLANTIQUE**

De février à juin 1979, le N.O. « Meteor » a exécuté dix sections dans l'Atlantique équatorial le long de 22° W entre 3° N et 2° S. Pendant une partie de celle période des courantomètres ont été mouillés. Les données récoltées sont utilisées pour étudier l'étalement vertical des isolignes, caractéristique de la thermocline équatoriale. Deux mécanismes peuvent expliquer ce phénomène: l'augmentation du mélange vertical par le cisaillement entre le Courant Équatorial Sud et le Sous-Courant Équatorial ou la circulation méridienne associée à l'upwelling équatorial. Leur importance relative est comparée en calculant les différents termes de l'équation de la conservation de la chaleur. Il

(1) Institut für Meereskunde, Düsternbrooker Weg 20, D-2300 Kiel 1, F. R. Germany.

en résulte que le mélange vertical est suffisamment intense pour équilibrer le gain de chaleur de l'océan, mais qu'il reste constant pendant les périodes à fort ou faible étalement thermoclinal parce que l'accroissement du coefficient de mélange vertical est compensé par une diminution de la dérivée seconde de la température. Cela signifie que l'advection verticale est nécessaire pour expliquer les variations de l'étalement de la thermocline et celles de la température de surface. La vitesse verticale est déduite du calcul de la divergence horizontale en supposant, pour estimer sa composante zonale, que le courant fluctue avec une période de 25 jours. La vitesse verticale ainsi calculée est trop élevée et doit être corrigée pour rendre compte des variations réelles de température. On arrive alors à une vitesse de 3,4 m.j⁻¹ pendant une période d'upwelling. On peut finalement conclure que le mélange vertical induit en permanence un étalement équatorial de la thermocline qui est accru par l'advection verticale en période d'upwelling.

MOTS-CLÉS : Upwelling équatorial — Écartement de la thermocline — Mélange vertical — Advection verticale — Mesures de STD, sels nutritifs et courants.

ZUSAMMENFASSUNG

DIE VERÄNDERLICHKEIT DER SPRUNGSCHICHTAUFSPREIZUNG ALS HINWEIS AUF ÄQUATORIALEN AUFTRIEB IM ATLANTISCHEN OZEAN

Von Februar bis Juni 1979 wurden mit dem F.S. « Meteor » zehn hydrographische Schnitte im äquatorialen Atlantik entlang 22°W zwischen 2°S und 3°N ausgeführt. Während eines Teiles dieser Zeit waren Strömungsmesser-verankerungen ausgebracht. Dieser Datensatz wird dazu benutzt, um die vertikale Aufspreizung der Isolinien im Sprungschichtniveau zu untersuchen, die in den äquatorialen Ozeanen beobachtet wird. Zwei Mechanismen stehen zur Verfügung, um diese Beobachtung zu erklären: Die meridional zunehmende vertikale Vermischung infolge der starken Scherung zwischen dem Südäquatorialström und dem Äquatorialunterstrom oder meridionale Zirkulationszellen, die zum Auftrieb am Äquator führen. Durch die Abschätzung der einzelnen Terme in der Wärmeerhaltungsgleichung und der Anpassung des Ergebnisses an die beobachtete zeitliche Temperaturveränderung wird die Bedeutung der einzelnen Prozesse miteinander verglichen. Es zeigt sich, dass vertikale Vermischung zu einem mittleren vertikalen Wärmetransport führt, der gross genug ist, um den Wärmegewinn des Ozeans zu kompensieren. Die Bedeutung der vertikalen Vermischung zu Zeiten starker oder schwacher Aufspreizung bleibt jedoch gleich, da ein zunehmender Vermischungskoeffizient durch eine abnehmende zweite vertikale Ableitung der Temperatur ausgeglichen wird. Es wird gefolgert, daß äquatorialer Auftrieb nötig ist, um die verstärkte Aufspreizung der Isolinien zu erklären. Da Strömungsmessungen nur auf einem meridionalen Schnitt zur Verfügung stehen, muss die Berechnung der horizontalen Divergenz unter Zuhilfenahme der Eigenschaften einer hypothetischen äquatorialen Welle mit einer Periode von 25 Tagen erfolgen. Die berechnete Vertikalgeschwindigkeit ist zu hoch und wird an die beobachtete zeitliche Temperaturveränderung angepasst. Es ergibt sich eine Vertikalgeschwindigkeit von 3,4 m/d während eines Auftriebsereignisses.

SCHLÜSSELWÖRTER : Äquatorialer Auftrieb — Sprungschichtaufspreizung — Vertikale Vermischung — Vertikale Advektion — STD-, Nährstoff- und Strömungsmessungen.

INTRODUCTION

A tongue of cold surface water in the equatorial Atlantic has been known since the early days of marine research (e.g. SCHOTT, 1902). The cooling is most intense in the Gulf of Guinea and decreases to the west; it is strongest in the boreal summer. The horizontal advection from the Southwest-African Upwelling area was given as the reason. With the data from the "Meteor"-cruise 1925-1927, DEFANT (1936) investigated the features of the equatorial current system. He deduced meridional circulation cells with upward movement at the equator. Equatorial upwelling could be explained

by the change of sign of the Coriolis force at the equator. After the rediscovery of the Equatorial Undercurrent (CROMWELL *et al.*, 1954, VOIGT, 1961), the high vertical shear due to the jet-like structure of the Equatorial Undercurrent was accepted as a further mechanism to transport cooler water by vertical mixing to the surface. This assumption is consistent with the observed seasonal cycle in the surface cooling since it is known (KATZ *et al.*, 1977) that the zonal pressure gradient which drives the Equatorial Undercurrent is subject to a seasonal cycle as well.

Various authors have discussed the influence of the different processes (e.g. VOITURIEZ and

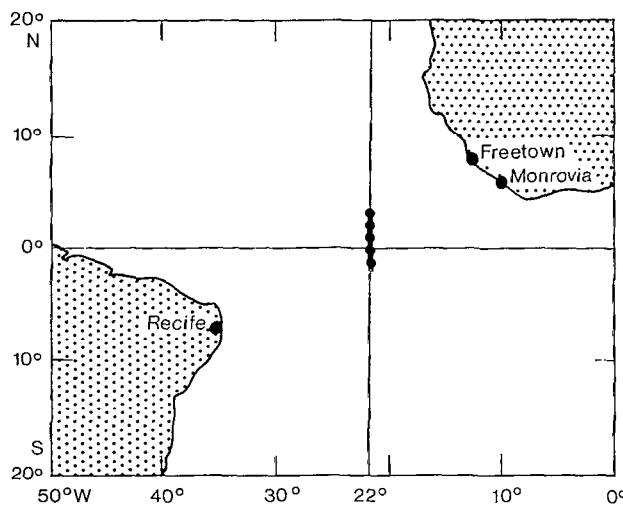


FIG. 1. — The area of observations with R. V. "Meteor" during FGGE-Equator '79'. The dots indicate current meter moorings. Along the line, STD-measurements and nutrient casts were carried out

La région des opérations du N. O. « Meteor » pendant les campagnes « FGGE-Equator 79 ». Les points indiquent les mouillages de courantomètres. Sur la section furent exécutées des mesures STD et des prélèvements d'eau pour l'analyse des sels nutritifs

HERBLAND, 1982). Nevertheless there is not yet a convincing data set published to quantify them. The major reason for this is that the ratio of meridional to zonal velocity and the ratio of mean to standard deviation of the meridional velocity is about 1/5. It was one of the aims of the R.V. "Meteor"-cruise ("FGGE-Equator '79") to provide a suitable data set to obtain further insight in this problem.

THE DATA

From 27 January to 23 June 1979, R.V. "Meteor", working in the FGGE project, surveyed the central equatorial Atlantic on a section along 22° W from 30° N to 2° S (fig. 1). The hydrographic section was repeated ten times (fig. 2). A continuous STD and a rosette sampler for nutrient casts were used. Five current meter moorings were deployed on the line (fig. 1). Taut wire techniques with surface buoys were used in order to measure wind and near surface currents. At 15 m depth VAGM's (sampling interval 7.5 min) and, at deeper depths, Aanderaa current meters (sampling interval 30 min.) were used. The equatorial mooring released itself after four days and was reinstalled at 10 February. At 1° S only one instrument could be recovered. Because of wire corrosion all moorings had to be removed at the end of March, yielding record lengths between 40 and 55 days. Only two moorings could be reinstalled from May to June at 0° and 2° N with a record length of 40 and 43 days respectively. During

the whole experiment five instruments lost their rotors and ten failed for different technical reasons (BAUERFEIND *et al.*, *in prep.*).

THE SPREADING OF THE ISOLINES

Comparisons between the nutrient distributions reveal some general features which are consistent with the temperature distributions (fig. 3). We can distinguish between three layers :

- - a nutrient poor and warm near-surface mixed layer;

- - a transitional layer with high vertical gradients. The vertical gradients vary along the section with a minimum near the equator;

- - a deep layer with small vertical gradients, lower temperature and high nutrient content.

Our main interest is in the transitional layer because physical processes there control the heat withdrawl from the surface mixed layer and the nutrient supply into the euphotic zone. The Equatorial Undercurrent is confined to this layer. Figure 4 shows the mean zonal current as measured from 31 January to 30 March 1979 along 22° W and the transitional layer. It is obvious that the definition of the same layer by temperature or concentration of nutrients is somewhat arbitrary, if one takes into account that the sources and sinks are of a different character. Nevertheless, since biological nutrient consumption and heating are due to the penetration of sunlight into the near surface layer

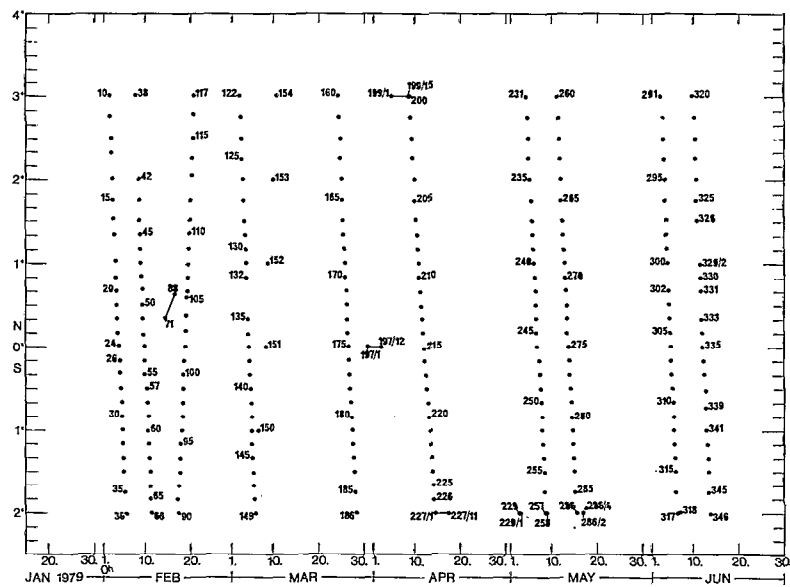


FIG. 2. — The time and meridional distribution of the STD-measurements and nutrient casts
Répartition mérienne et temporelle des stations hydrologiques

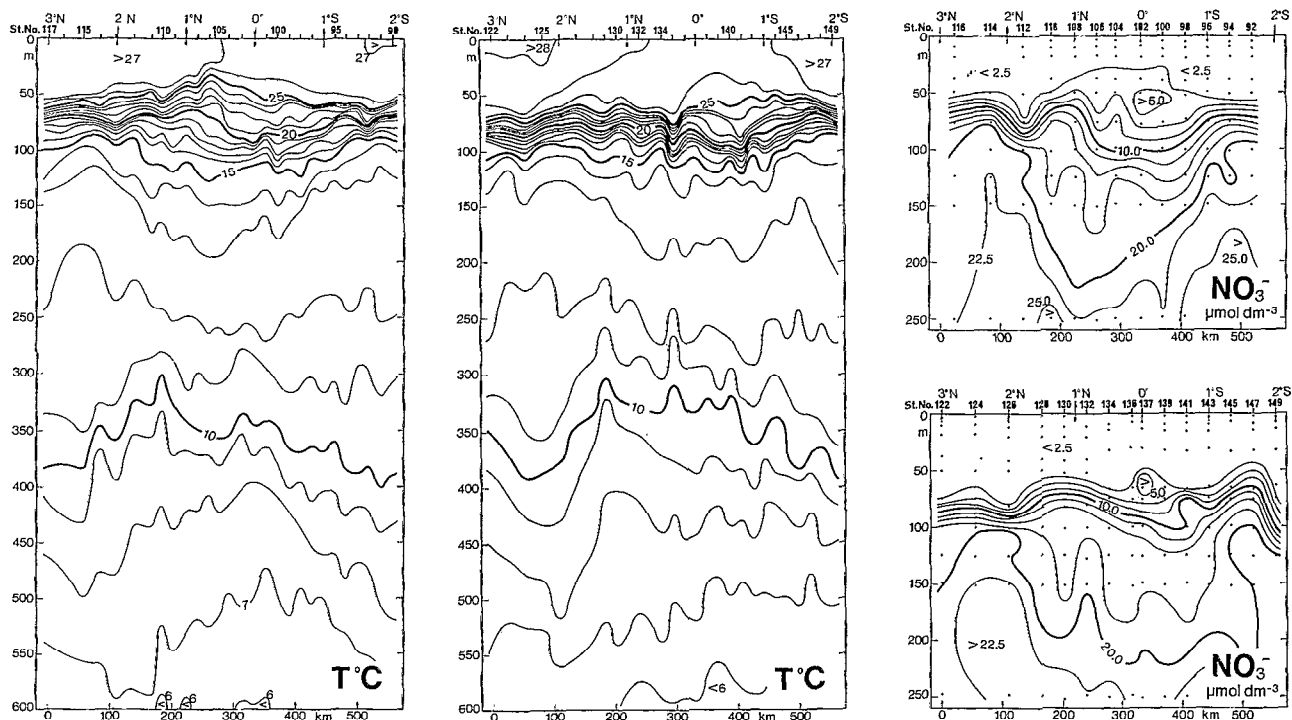


FIG. 3. — Temperature and nitrate on a section along 22° W carried out from 17 to 20 February 1979 (St. 90-117) and from 2 to 6 March 1979 (St. 122-149)

Sections de température et de nitrate faites le long de 22° W du 17 au 20 février 1979 (St. 90-117) et du 2 au 6 mars 1979 (St. 122-149)

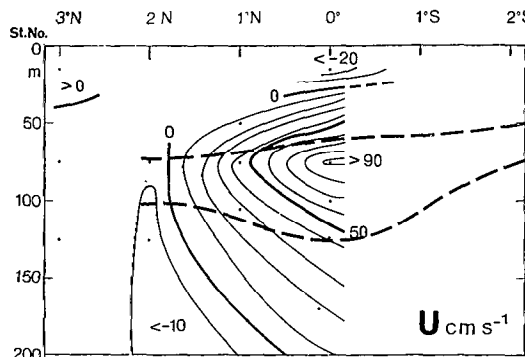
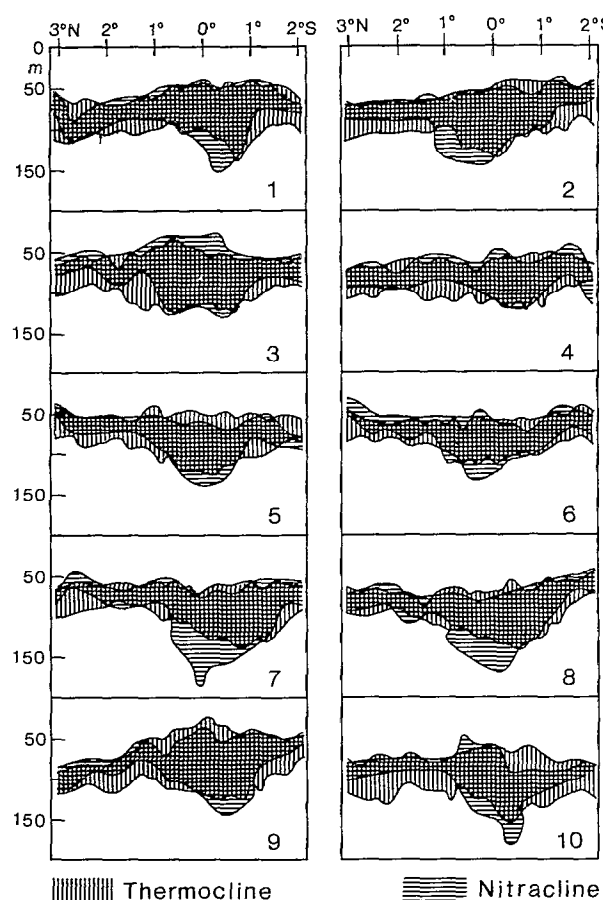


FIG. 4. — A section along 22° W showing the mean zonal current between 31 January and 30 March 1979 (positive to the east) and the schematic location of the thermocline, defined by the average position of the 25 °C and 15 °C isotherms

Le courant zonal moyen du 31 janvier au 30 mars 1979 (positif vers l'est) et la localisation schématique de la thermocline, définie par la position moyenne des isothermes 25 °C et 15 °C

FIG. 5. — The variability of the thermocline (defined between 25 °C and 15 °C) and the nitracline (defined between 2.5 μ mol dm⁻³ and 15.0 μ mol dm⁻³) during the period from 27 January to 13 June 1979. The time of the individual section is given in Figure 2

Variabilité de la thermocline (définie entre 25 °C et 15 °C) et de la nitracline (définie entre 2.5 μ mole dm⁻³ et 15 μ mole dm⁻³) pendant la période du 27 janvier au 13 juin 1979. Les dates des sections sont données en figure 2



and since the exchange with deeper layers is based on the same physical processes, the comparison seems reasonable to us. It is possible to define the transition from the mixed layer to the thermocline by the vertical gradient or a fixed temperature. In our data no significant difference was found between the methods. We have therefore chosen the thermocline defined between 25 °C and 15 °C and the nitracline defined between 2.5 and 15 μ mol dm⁻³ to show the extent and the variability of the transition layer (fig. 5). There are two reasons which do not permit one to interpret this figure as a time sequence. First, because of the high advection rates (25 cm s⁻¹ to the west at 15 m in the South Equatorial Current and 100 cm s⁻¹ to the east at 75 m in the Equatorial Undercurrent) and an average time lag between two sections of ten days, subsequent sections must be considered as showing the consequences of processes up to 900 km apart. Second, the temperature time series of the moored instruments indicate energetic events on a time scale less than five days which can easily occur between

two subsequent sections. We therefore treat the sections as independent samples and try to explain some typical features with the help of the current meter data which are recorded during the time of the section.

In Figure 5, periods with strong and weak isoline spreading are seen. We choose section 3 as an example of strong spreading with a cool and nutrient rich surface layer because it was carried out during a period of mixed layer cooling of 0.25 K/d over five days (fig. 6). The mean NO₃⁻-concentration in the upper ten meters within 20 nms of the equator was 0.76 μ mol dm⁻³. Section 4 was chosen as an example for a warm and nutrient poor surface layer corresponding to weak spreading. It was carried out after a period of warming lasting for three days with 0.18 K/d. The NO₃⁻-concentration fell to 0.25 μ mol dm⁻³. The cool situation is more pronounced during section 9 than in section 3, but at this time only very few current meter measurements are available.

The moored current meter records corresponding

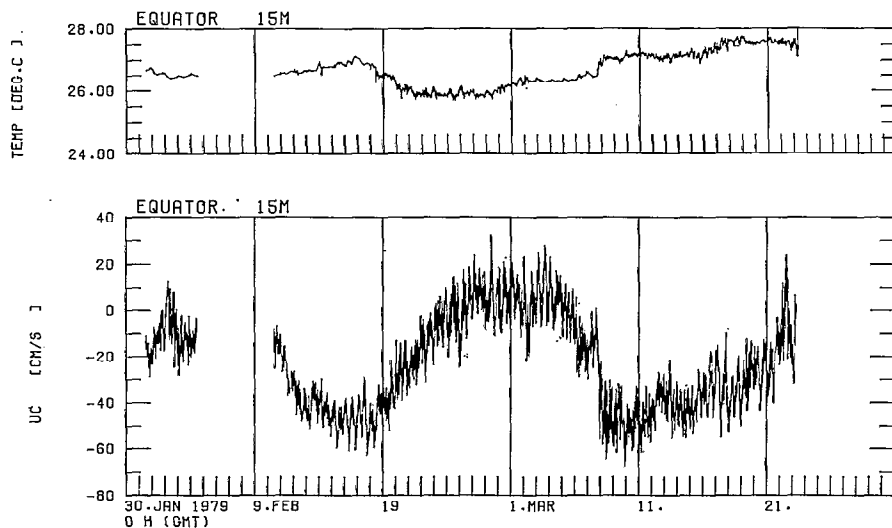


FIG. 6. — Time series of the temperature and the zonal component of the current at the equator at 15 m depth.

Série temporelle de la température et du courant zonal à l'équateur à la profondeur 15 m

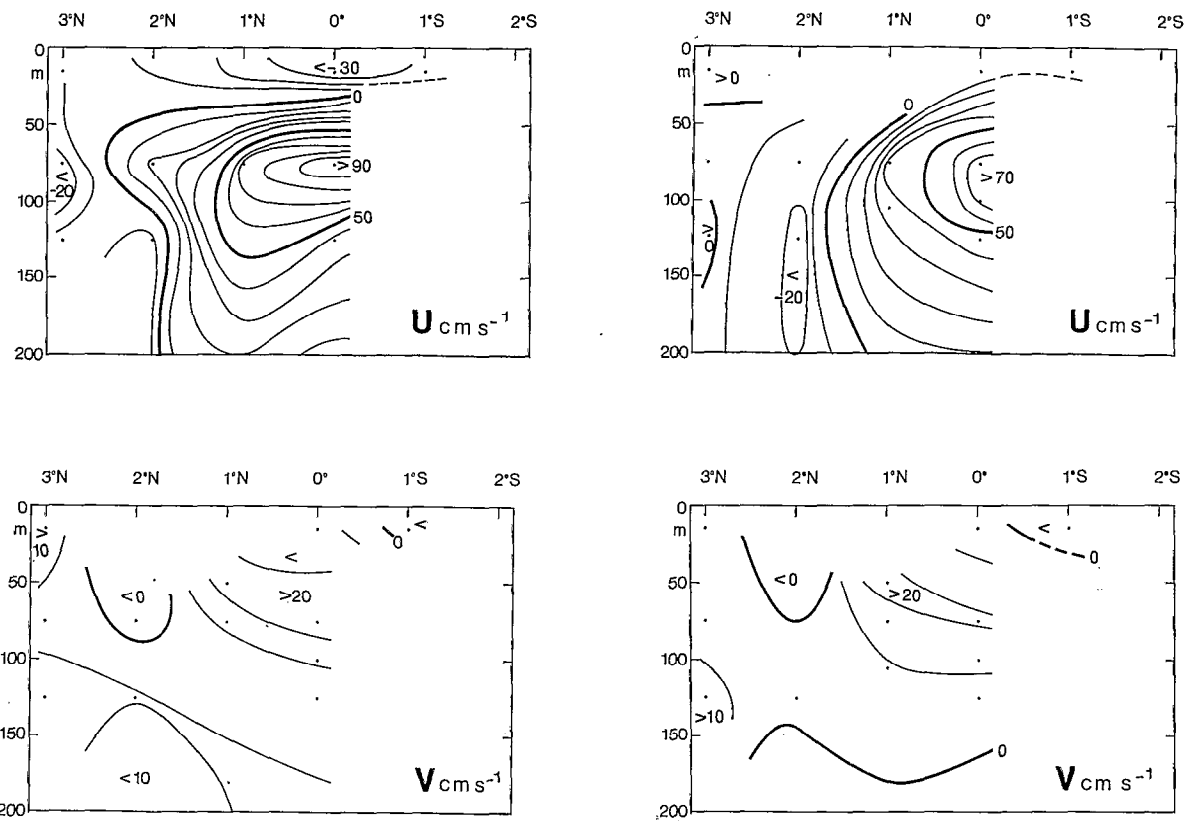


FIG. 7. — The mean currents measured during section 3, 17 to 20 February 1979, left, and section 4, 2 to 6 March 1979, right
(u positive to the east, v positive to the north)

Les courants moyens mesurés pendant la section 3 du 17 au 20 février 1979 (à gauche) et la section 4 du 2 au 6 mars 1979 (à droite); u est positif vers l'est, v est positif vers le nord

to section 3 and 4 are depicted in figure 7 as averages over the time which was needed to carry out the sections. It is to be seen that the vertical current shear and the horizontal divergence are changing by about a factor of two.

The extent to which vertical mixing or advection can contribute to these observations, is worked out below by means of the available data.

THE ESTIMATE OF VERTICAL MIXING

For the quantification of the vertical mixing, it is necessary to calculate a turbulent vertical mixing coefficient. This coefficient can be deduced from the balance of mean kinetical turbulent energy.

Under the assumption that a local balance of the mean turbulent kinetic energy exists between the generation by the shear of the mean velocity field, and the loss due to the stratification, turbulent diffusion and dissipation, the following equation results:

$$\overline{u'w'} \frac{\partial \bar{u}}{\partial z} (1 - \sigma Rf) = \epsilon \quad (\text{MONIN and YAGLON, 1971})$$

with u' , w' : turbulent velocity components

\bar{u} : mean horizontal velocity

z : vertical coordinate

g : acceleration of gravity

ρ : density

$$Rf = \frac{\frac{g}{\rho} \overline{u'w'}}{\overline{u'w'} \frac{\partial \bar{u}}{\partial z}} : \text{Flux Richardson number}$$

The generation is given as $\overline{u'w'} \frac{\partial \bar{u}}{\partial z}$.

The loss due to stratification is assumed to be proportional to the generation $\frac{g}{\rho} \overline{u'w'} = Rf \overline{u'w'} \frac{\partial \bar{u}}{\partial z}$.

The loss due to turbulent diffusion is assumed to be proportional to the loss due to stratification with a factor of $\sigma - 1$. We adopted $\sigma = 5$ (MONIN and YAGLON, 1971).

The dissipation ϵ is assumed to be locally constant.

After the introduction of the semi-empirical formula $\overline{u'w'} = K_m \frac{\partial \bar{u}}{\partial z}$.

K_m : vertical turbulent diffusion coefficient for momentum.

$$\text{one can calculate } K_m = \frac{\epsilon}{(1 - \sigma Rf) \left(\frac{\partial \bar{u}}{\partial z} \right)^2}.$$

Above the core we calculated:

$$Ri = \frac{N^2}{\left(\frac{\partial \bar{u}}{\partial z} \right)^2} = 0.9 : \quad \text{Gradient Richardson number, with the assumption } \frac{\partial \bar{u}}{\partial z} >> \frac{\partial \bar{v}}{\partial z} \quad (N^2 : \text{Brunt-Väisälä-frequency}).$$

$$\frac{\partial \bar{u}}{\partial z} = 1.9 \cdot 10^{-2} \text{ s}^{-1} : \quad 40 \text{ d mean vertical shear between the } 75 \text{ m and } 15 \text{ m depths at the equator.}$$

$$Rf = \alpha Ri$$

$$\alpha = \frac{K_b}{K_m} = \frac{(1 + 5 Ri)}{(1 + 5.77 Ri)^2} = 0.14 \quad (\text{JONES, 1973})$$

$$K_b : \text{turbulent diffusion coefficient of a dissolved substance.}$$

α was measured by ELLISON and TURNER (1960) with tank experiments. Jones used this formula, but we cannot use the rest of his method to calculate the turbulent diffusion coefficients because our current meter distance of 60 m does not allow for his assumption of constant stress.

Below the core we calculated:

$$Ri = 2.1$$

$$\frac{\partial \bar{u}}{\partial z} = 1.0 \cdot 10^{-2} \text{ s}^{-1} : \quad 40 \text{ day mean vertical shear between the } 125 \text{ m and } 75 \text{ m depths at the equator.}$$

$$\alpha = 0.06$$

The dissipation rates of $\epsilon = 4 \cdot 10^{-3} \text{ cm}^2 \text{ s}^{-3}$ above and $\epsilon = 0.5 \cdot 10^{-3} \text{ cm}^2 \text{ s}^{-3}$ below the core are the averages of values in Table 2 in CRAWFORD and OSBORN, 1980a. They also calculated turbulent diffusion coefficients, which we cannot use because they neglected the buoyancy term in their estimates. This is not possible in our observations. K_m is calculated with the given formula as a mean over 40 days. If the shear increases the stationary balance is disturbed and the derived equation is no longer valid, otherwise increasing shear would decrease the mixing coefficients. We avoid this problem by

$$\text{assuming a linear dependence } K_m = l^2 \left(\frac{\partial \bar{u}}{\partial z} \right) \quad (\text{MONIN and YAGLON, 1971}),$$

and l^2 , the mixing length, taken as constant and calculated from the mean K_m and the mean vertical velocity gradient. The resulting coefficients and the corresponding terms in the equation of heat conservation are given in Table I as 40 day means over the first mooring period and 3.5 day means of the two sections to be compared.

While looking at the numbers, it must be kept in mind that the simplifications which are necessary to deduce the formulas are difficult to control and

TABLE I

Estimates of vertical turbulent diffusion coefficients and the resulting mixing term in the equation of heat conservation at 45 m and 100 m depths at the equator

Estimation des coefficients de diffusion verticale turbulente et du terme de mélange dans l'équation de conservation de la chaleur à 45 et 100 m, à l'équateur

	mean 10 Feb.-30 March	cold section 17-20 Feb.	warm section 2-6 March
K_b (cm ² /s).....	4.3	5.1	2.7
45 m $\frac{\partial^2 T}{\partial z^2}$ (K/cm ²).....	— 0.4 · 10 ⁻⁶	— 0.2 · 10 ⁻⁶	— 0.4 · 10 ⁻⁶
$K_b \frac{\partial^2 T}{\partial z^2}$ (K/d)	— 0.14	— 0.09	— 0.10
100 m K_b (cm ² /s)	0.9	1.1	0.5
100 m $\frac{\partial^2 T}{\partial z^2}$ (K/cm ²).....	0.3 · 10 ⁻⁶	0.3 · 10 ⁻⁶	0.7 · 10 ⁻⁶
100 m $K_b \frac{\partial^2 T}{\partial z^2}$ (K/d)	0.02	0.03	0.04

probably result in a much higher error than instrumental errors or signal to noise ratios could produce. An error calculation is carried out under the assumption that the error propagation is gaussian. We find that ΔK_b is most sensitive to $\Delta \varepsilon$, $\Delta \sigma$ and ΔR_f . ΔR_f is most sensitive to $\Delta \alpha$. We estimated $\Delta \alpha = \pm 0.05$ as a reasonable standard deviation by varying R_f in the observed range. We find $\Delta R_f/R_f = 37\%$. From the CRAWFORD and OSBORN, 1980a, we calculated $\Delta \varepsilon = \pm 2 \text{ cm}^2 \text{ s}^{-3}$. The value $\Delta \sigma = \pm 2$ is chosen arbitrarily because no data exist. A relative error of 40 % seems realistic to us to test the sensitivity of the results using this parameter. Nevertheless the assumption of a gaussian distribution of $\Delta \sigma$ is doubtful. Therefore, we calculated the lower limit of ΔK , not by the gaussian error propagation but under the assumption of $\sigma = 1$, which means no turbulent transport of mean kinetic energy.

We find $\Delta K_b/K_b = +98\%/-47\%$. In Table II this range is compared with the estimates of other authors.

The agreement of the results derived under different assumptions and with different methods, suggests that the result does not depend critically on the various assumptions.

The effect of vertical mixing on the temperature at a given level is calculated by means of the corresponding term in the equation of heat conservation. The results are shown in Table I. The second derivatives of temperature are calculated from five profiles at the equator during 40 days. In the levels where temperature time series exist from the moored current meters the difference to the profiles stay within ± 0.1 K. The resulting uncertainty is much smaller than that of K_b . It turns out that there is no significant time change of local temperature

TABLE II

Range of calculated turbulent diffusion coefficients (K_m for momentum, K_b for dissolved substances) in comparison with other authors. F. & B.: our values; C. & O.: CRAWFORD and OSBORN, 1980d; K. et al.: KATZ et al., 1980

Intervalle des coefficients de diffusion turbulente calculés (K_m pour la quantité de mouvement, K_b pour les substances dissoutes) comparé aux évaluations d'autres auteurs. F. et B.: nos valeurs; C. et O.: CRAWFORD et OSBORN, 1980b; K. et al.: KATZ et al., 1980

	K_m (cm ² s ⁻¹) F. & B. C. & O.	K_b (cm ² s ⁻¹) F. & B. K. et al.
Above the EUC core.....	15-60 0.5-100	2-9 1.5
Below the EUC core.....	3-12 0.2-10	0-2 1

due to vertical mixing because the increased mixing coefficient during the cold section is balanced by a decrease of $\frac{\partial^2 T}{\partial z^2}$. We conclude that vertical advection must contribute to explain the observed cooling in the mixed layer.

THE ESTIMATION OF VERTICAL ADVECTION ON THE BASIS OF HORIZONTAL DIVERGENCE

As there is no significant change of vertical mixing which can explain the increase of isoline spreading, we now investigate vertical advection. According to various earlier authors (e.g. CHARNEY and SPIEGEL, 1971), we except meridional circulation cells which are centered at the equator or slightly south of it. There should be a divergence above the core of the Equatorial Undercurrent and a convergence in the core. With a suitable deployment of current meters it should be possible to calculate the vertical velocity due to the meridional cells from the observed horizontal divergence using the continuity equation. However, with our current meter locations, we have two major problems:

- above the core, we have current meters at 15 m depth at 1° S and at the equator; in the core at 75 m at 1° N and at the equator;

- we have only measurements along a meridional section.

Thus, we cannot associate the shallow divergence with the deep convergence. Furthermore, it is not possible to show if the cells exist on both sides of the equator. The location of the salinity core associated with the Equatorial Undercurrent indicates its mean location during the observation period south of the equator (SY and MEINCKE, 1981). Therefore we assume that our measurements between

1° S and the equator include the most important part of the divergence region.

Furthermore, the core of the Equatorial Undercurrent fluctuates meridionally, as is well known (e.g. DÜING *et al.*, 1975). Due to the fluctuations, the core velocity is, in general, not zonal. For this reason meridional velocity gradients which are important can be observed, but they might be completely balanced by the zonal component. Therefore we can only expect to calculate reasonable vertical velocities from the measured meridional divergence for times scales long enough to average out the undercurrent fluctuations. The zonal divergence is calculated using the assumption that the most intense current fluctuations, which generate the zonal variability, are caused by a westward propagating wave with a period of 25 days (fig. 6) and a wave length of the order of 1000 km (PHILANDER and DÜING, 1980). It should be kept in mind that there are several different waves with different wave-lengths superimposed. The one wave assumption is therefore a very simple one.

To test if the calculated divergences differ significantly from zero, a different approach has to be chosen for the 40 day and 3.5 day means. The variance of the 40 day time series is dominated by low frequency fluctuations; that of the 3.5 day time series by the tides. We therefore calculated the effective number of samples N_{eff} of the 40 day time series from the autocorrelation function (e.g. TAUBENHEIM, 1969). For the 3.5 day time series we calculated mean values over 12.4 or 24.8 hours to eliminate the tides. In order to receive four samples of the 24.8 hours mean values we used 4.1 day time series. We accepted these values as independent samples under the assumption that the period of the low frequency fluctuation is long enough that we can neglect the trend. The error calculations are summarized in Table III. It turns out, that

TABLE III

Calculation of 95 % confidence limits of the meridional velocity component. σ_{LP} : Standard deviation of the low passed or averaged time series; σ_0 : Standard deviation of the original time series; N_{eff} : Number of statistically independent samples; Δv : 95 % confidence interval of the mean value given by a t-test

Calcul des intervalles de confiance (niveau 95 %) de la composante méridienne de la vitesse. σ_{LP} : écart type des mesures filtrées (passé bas) ou moyennées ; σ_0 : écart type des mesures originales ; N_{eff} : nombre d'échantillons statistiquement indépendants ; Δv : Intervalle de confiance au niveau 95 % de la valeur moyenne (test t)

	mean		cold section		warm section	
	1° S	EQ	1° S	EQ	1° S	EQ
σ_{LP}/σ_0	0.93	0.93	0.47	0.66	0.41	0.40
σ_{LP} (cm/s).....	11.6	14.9	3.1	5.5	3.1	2.4
N_{eff}	5	5	7	4	4	7
Δv (cm/s).....	16.1	20.7	2.8	7.6	4.3	2.2

TABLE IV

Estimates of vertical advection from horizontal divergence, w_m is the vertical velocity calculated only from the measured meridional divergence, z is positive downward

Estimations de l'advection verticale à partir de la divergence horizontale; w_m est la vitesse verticale calculée à partir de la divergence méridienne; z est positif vers le bas

	mean 10 Feb.-30 March	cold section 17-20 Feb.	warm section 2-6 March
$\frac{\partial v}{\partial y}$ (cm s ⁻¹ /km).....	2.5/111.1	18.1/111.1	10.6/111.1
w_m (m/d).....	— 0.9	— 6.3	— 3.7
$\frac{\partial u}{\partial x}$ (cm s ⁻¹ /km).....	—	17/111.1	— 17/111.1
w (m/d).....	— 0.9	— 12.2	2.2
$\frac{\partial T}{\partial z}$ (K/m).....	— 5.6/60	— 4.9/60	— 5.0/60
— $w \frac{\partial T}{\partial z}$ (K/d).....	— 0.08	— 1.00	0.18

TABLE V

Estimated terms of the conservation of heat equation in K/d. The errors are only given for the mean values, because the necessary assumptions to calculate them produce a higher uncertainty than the calculated variations

Valeurs estimées des termes de l'équation de conservation de la chaleur en K/d. Les erreurs sont données seulement pour les valeurs moyennes, parce que les hypothèses nécessaires à leur calcul produisent une incertitude plus grande que les variations calculée

	mean 10 Feb.-30 March	cold section 17-20 Feb.	warm section 2-6 March	error
— $u \frac{\partial T}{\partial x}$	0.01	0.01	0.01	± 0.01
— $v \frac{\partial T}{\partial y}$	0.02	0.10	0.03	± 0.02
— $w \frac{\partial T}{\partial z}$	— 0.08	— 1.00	+ 0.19	± 0.10
$K_R \frac{\partial^2 T}{\partial y^2}$	0.01	— 0.03	0.05	± 0.08
$K_b \frac{\partial^2 T}{\partial z^2}$	— 0.14	— 0.09	— 0.10	{ + 0.10 — 0.05
Q	0.04	0.04	0.04	± 0.01
$\frac{\partial T}{\partial t}$ calculated	— 0.14	— 0.97	0.22	± 0.16
$\frac{\partial T}{\partial t}$ observed	0.02	— 0.25	0.18	± 0.08
W_{cor} (m/d).....	+ 0.90	— 3.4	+ 1.80	± 1.7 m/d

only the cold sections show a divergence which differs significantly from zero. We find from the equation of continuity,

$$w(45 \text{ m}) = \int_0^{45 \text{ m}} \left(-\frac{\partial u}{\partial x} - \frac{\partial v}{\partial y} \right) dz,$$

that the vertical velocity is upward during section 3 and not significantly different from zero during section 4. The integration is done assuming constant derivatives. The calculated values are summarized in Table IV. The vertical velocity which results from the meridional divergence is given as w_m .

We conclude from these numbers, that the vertical advection is the dominant mechanism to increase the spreading of isolines during the cold section. Nevertheless the calculated vertical velocity of 12 m/d seems too high. To check this number we tried to calculate the different terms of the local heat balance.

THE HEAT BALANCE

The local heat balance is given by the conservation of heat equation:

$$\frac{\partial T}{\partial t} + u \frac{\partial T}{\partial x} + v \frac{\partial T}{\partial y} + w \frac{\partial T}{\partial z} = K_u \left(\frac{\partial^2 T}{\partial x^2} + \frac{\partial^2 T}{\partial y^2} \right) + K_b \frac{\partial^2 T}{\partial z^2} + Q$$

The estimate is summarized in Table V. The calculations are done on the basis of the following data:

- $u \frac{\partial T}{\partial x}$: u from the current meter at 15 m at the equator
 $\frac{\partial T}{\partial x}$ = const. from PHILANDER and DURING, 1980.
- $v \frac{\partial T}{\partial y}$: v from the current meter at 15 m at the equator
 $\frac{\partial T}{\partial y}$ from hydrographic sections.
- $w \frac{\partial T}{\partial z}$: from current meter at 15 m and 75 m at the equator (Table IV).
- $K_u \frac{\partial^2 T}{\partial x^2} < < u \frac{\partial T}{\partial x}$.
- $K_H \frac{\partial^2 T}{\partial y^2}$: $K_H = 2.10^7 \text{ cm}^2 \text{ s}^{-1}$ (KATZ *et al.*, 1980).
- $\frac{\partial^2 T}{\partial y^2}$: from hydrographic sections.
- K_b : from Table II.
- Q : HASTENRATH and LAMB, 1977.
The monthly mean heat gain was assumed to be equally distributed over a 45 m deep mixed layer.

The errors in Table V are calculated from the error estimates of the individual data or from the

observed variance of the used time series under the assumption of a propagating gaussian error.

Our first approach was to calculate a local time change of temperature from the sum of the estimated terms. The comparison with the observed time change shows a marked discrepancy for the cold section. Therefore we calculated a corrected vertical velocity w_{cor} in order to fit the observed time change. The resulting $w = -3.4 \pm 1.7 \text{ m/d}$ is significantly different from zero, but three times smaller than the one which we deduced by means of the wave hypothesis. The vertical velocities for the warm section and the mean over 40 days are not significantly different from zero. This confirms that a mean spreading, which is present due to vertical mixing, is increased during cold periods by vertical advection.

CONCLUSIONS

From these calculations it can be seen, that the vertical advection exceeds the turbulent transport in times of observed "upwelling". The turbulent transport is about 3 times larger in the surface layer than in the thermostad. There is no considerable time variance. We conclude that a steady nutrient supply into the euphotic zone is driven by the undercurrent shear.

Since the second derivative of temperature decreases with increasing shear, no local change of temperature occurs with increasing mixing coefficient. Therefore an increasing upward velocity is necessary to produce an upwelling event. This may be due to the local wind (the observed winds are more favourable to upwelling at section 3 [SPETH *et al.*, *in prep.*]) or to undercurrent dynamics. The undercurrent is observed to be strongest and furthest to the north during section 3 (fig. 7). It must be taken into account that the vertical velocity cannot be calculated from a purely two dimensional balance.

There is evidence of two upwelling periods during our observations, in February and in June (in the monthly mean data (MERLE *et al.*, 1980) this appears only north of 5° N). The June upwelling period concurs with the beginning of the more pronounced summer cooling. It cannot be treated in the same way as section 3 because not enough current meter measurements are available. The small mean core velocity of 73 cm s⁻¹ gives an indication that the shear and the consequential turbulent transport do not exceed the one at section 4. In contrast, the winds are much higher (SPETH *et al.*, *in prep.*) leading to enhanced upwelling. At both periods a cooling of the euphotic layer is correlated with the increase of nutrient concentration. The chlorophyll-a content of a water column below one square

meter is 1.5 times higher during section 3 than during section 4. The comparison of sections 9 and 4 gives a factor of 3 (MEYERHÖFER, 1980). The zooplankton samples do not reflect the event-like upwelling at section 3 but they show a clear signal at section 9 (ROLKE, 1981). This gives an indication to the biological consequences of the undercurrent dynamics.

ACKNOWLEDGEMENTS

This research was supported by the Deutsche Forschungsgemeinschaft. We are grateful to Mrs PETERSEN and Mr EISELE for preparing the drawings and Mrs SCHUSTER for typing the manuscript.

Manuscrit reçu au Service des Éditions de l'O.R.S.T.O.M., le 13 mai 1982

REFERENCES

- BAUERFEIND (E.), BROCKMANN (C.), FAHRBACH (E.), MEINCKE (J.), ROHARDT (G.) and SY (A.), *in prep.* — A compendium of the oceanographic data measured during the "FGGE-Equator '79"—Cruise of RV "Meteor".
- CHARNEY (J. G.) and SPIEGEL (S. L.), 1971. — Structure of wind-driven equatorial currents in homogeneous Oceans. *J. Phys. Oceanogr.*, 1 : 149-160.
- CRAWFORD (W. R.) and OSBORN (T. R.), 1980a. — Microstructure measurements in the Atlantic Equatorial Undercurrent during GATE. *Deep-Sea Res.*, 26 (Suppl.) : 285-308.
- CRAWFORD (W. R.) and OSBORN (T. R.), 1980b. — Energetics of the Atlantic Equatorial Undercurrent. *Deep-Sea Res.*, 26 (Suppl.) : 309-323.
- CROMWELL (T.), MONTGOMERY (R. B.) and STROUP (E. D.), 1954. — Equatorial Undercurrent in the Pacific revealed by new methods. *Science*, 119 : 648-649.
- DEFANT (A.), 1936. — Die Troposphäre. Deutsche Atlantische Exped. "Meteor" 1925-1927, Wiss. Erg., Bd VI, Teil 1 (3) : 289-411.
- DUING (W.), HISARD (P.), KATZ (E.), MEINCKE (J.), MILLER (L.), MUROSHKIN (K. V.), PHILANDER (G.), RIBNIKOV (A. A.), VOIGT (K.) and WEISBERG (R.), 1975. — Meanders and long waves in the equatorial Atlantic. *Nature*, 257 : 280-284.
- ELLISON (T. H.) and TURNER (J. S.), 1960. — Mixing of dense Fluid in a turbulent pipe Flow, Part 2. Dependence of transfer coefficients on local stability. *J. Fluid Mech.*, 8 : 529-544.
- HASTENRATH (S.) and LAMB (P.), 1978. — Heat budget atlas of the tropical Atlantic and eastern Pacific Oceans. University of Wisconsin Press, Madison : 112 p.
- JONES (J. H.), 1973. — Vertical mixing in the Equatorial Undercurrent. *J. Phys. Oceanogr.*, 3 : 286-296.
- KATZ (E. J.), BELEVICH (R.), BRUCE (J.), BUBNOV (V.), COCHRANE (J.), DUING (W.), HISARD (P.), LASS (H. U.), MEINCKE (J.), DE MESQUITA (A.), MILLER (L.) and RYBNIKOV (A.), 1977. — Zonal pressure gradient along the equatorial Atlantic. *J. Mar. Res.*, 35 : 293-307.
- KATZ (E. J.), BRUCE (J. G.) and PETRIE (B. D.), 1980. — Salt and mass flux in the Atlantic Equatorial Undercurrent. *Deep-Sea Res.*, 26 (Suppl.) : 137-160.
- MERLE (J.), FIEUX (M.) and HISARD (P.), 1980. — Annual signal and interannual anomalies of sea surface temperature in the eastern equatorial Atlantic Ocean. *Deep-Sea Res.*, 26 (Suppl.) : 77-101.
- MEYERHÖFER (M.), 1980. — Ökologische Untersuchungen des Phytoplanktons im Äquatorialen Atlantik. Diplom-thesis, University of Kiel, 85 p.
- MONIN (A. S.) and YAGLOM (A. M.), 1971. — Statistical fluid mechanics: Mechanics of turbulence, Vol. 1, The MIT Press, Cambridge, Massachusetts, and London, 769 p.
- PHILANDER (S. G. H.) and DUING (W.), 1980. — The oceanic circulation of the tropical Atlantic, and its variability, during GATE. *Deep-Sea Res.*, 26 (Suppl.) : 1-27.
- ROLKE (M.), 1981. — Die Biomasse des kleineren Zooplanktons in den oberen 300 m des äquatorialen Atlantiks. Diplom-thesis, University of Kiel, 57 p.
- SCHOTT (G.), 1902. — Oceanographie und Maritime Meteorologie. Deutsche Tiefsee-Expedition "Valdivia" 1898-1899, Wiss. Erg., Bd I, 403 p.
- SPETH (P.), COLIN (C.) and KATZ (E.), *in prep.* — Wind data from buoys during FGGE.
- SY (A.) and MEINCKE (J.), 1981. — A comparison of hydrographic Features observed in the equatorial Atlantic during FGGE using a conventional CTD and a towed system. Recent Progress in Equatorial Oceanography: report of the final meeting of SCOR working group 47 in Venice, Italy, April 27-30, 1981, Nova University N.Y.I.T. Press: 55-60.
- TAUBENHEIM (J.), 1969. — Statistische Auswertung geophysikalischer und meteorologischer Daten. Akademische Verlagsgesellschaft Geest & Portig K.-G., Leipzig, 386 p.
- VOIGT (K.), 1961. — Äquatoriale Unterströmung auch im Atlantik (Ergebnisse von Strömungsmessungen auf einer atlantischen Ankerstation der "Michail Lomonosov" am Äquator im Mai 1959), *Beitr. Meereskunde*, 1 : 56-60.
- VOITURIEZ (B.) and HERBLAND (A.), 1982. — Comparison of the coastal and open ocean upwelling ecosystems of the tropical eastern Atlantic. *Rapp. P.-v. Réun. Cons. int. Explor. Mer.*, 180.